



## Cyanobacterial harmful algal blooms are a biological disturbance to western Lake Erie bacterial communities

Journal:	<i>Environmental Microbiology and Environmental Microbiology Reports</i>
Manuscript ID	EMI-2016-1463.R1
Journal:	Environmental Microbiology
Manuscript Type:	EMI - Research article
Date Submitted by the Author:	02-Dec-2016
Complete List of Authors:	Berry, Michelle; University of Michigan, Ecology and Evolutionary Biology Cory, Rose; University of Michigan, Earth and Environmental Sciences Davis, Timothy; NOAA-GLERL Duhaime, Melissa; University of Michigan, Ecology and Evolutionary Biology Johengen, Thomas; Cooperative Institute for Limnology and Ecosystem Research Kling, George; University of Michigan, Department of Ecology and Evolutionary Biology Marino, John; University of Michigan, Statistics Den Uyl, Paul Gossiaux, Duane; NOAA-GLERL Dick, Gregory; University of Michigan, Earth and Environmental Sciences Denef, Vincent; University of Michigan, Ecology and Evolutionary Biology
Keywords:	algae, microbial ecology, microbial communities, bacteria, resilience, community ecology

SCHOLARONE™  
Manuscripts

1 Cyanobacterial harmful algal blooms are a biological disturbance to western Lake Erie  
2 bacterial communities

3 Running title: Bacterial community ecology of CHABs

4  
5 **Michelle A. Berry<sup>1</sup>, Timothy W. Davis<sup>2</sup>, Rose M. Cory<sup>3</sup>, Melissa B. Duhaime<sup>1</sup>,**  
6 **Thomas H. Johengen<sup>4</sup>, George W. Kling<sup>1</sup>, John A. Marino<sup>1</sup>, Paul A. Den Uyl<sup>2</sup>, Duane**  
7 **Gossiaux<sup>3</sup>, Gregory J. Dick<sup>3,#</sup>, Vincent J. Denef<sup>1,#</sup>**

8  
9 <sup>1</sup>Department of Ecology and Evolutionary Biology, University of Michigan, Ann Arbor, MI,  
10 48109. <sup>2</sup>NOAA Great Lakes Environmental Research Laboratory, Ann Arbor MI, 48108

11 <sup>3</sup>Department of Earth and Environmental Sciences, University of Michigan, Ann Arbor, MI,  
12 48109. <sup>4</sup>Cooperative Institute for Limnology and Ecosystems Research, University of Michigan,  
13 Ann Arbor, MI, 48109.

14  
15 <sup>#</sup>Corresponding authors: 1141 Kraus Natural Science, 830 N. University, Ann Arbor, MI 48109,  
16 vdenef@umich.edu, Phone: +1 (734) 764-6481, Fax: +1 (734) 763-0544;  
17 gdick@umich.edu, Phone: +1 (734) 763-3228, Fax: +1 (734) 763-4690

18  
19  
20 Author contributions: GJD, VJD, THJ, TWD, MBD, GWK, RMC designed the experiment,  
21 MAB, JAM, TWD, DG, PD performed experiments, MAB analyzed data, and MAB, VJD, GJD,  
22 GWK, RMC, TWD, JAM wrote the paper.

23  
24

25 **Summary.**

26 Human activities are causing a global proliferation of cyanobacterial harmful algal  
27 blooms (CHABs), yet we have limited understanding of how these events affect  
28 freshwater bacterial communities. Using weekly data from western Lake Erie in 2014, we  
29 investigated how the cyanobacterial community varied over space and time, and whether  
30 the bloom affected non-cyanobacterial (nc-bacterial) diversity and composition.  
31 Cyanobacterial community composition fluctuated dynamically during the bloom, but  
32 was dominated by *Microcystis* and *Synechococcus* OTUs. The bloom's progression  
33 revealed potential impacts to nc-bacterial diversity. Nc-bacterial evenness displayed  
34 linear, unimodal, or no response to algal pigment levels, depending on the taxonomic  
35 group. In addition, the bloom coincided with a large shift in nc-bacterial community  
36 composition. These shifts could be partitioned into components predicted by pH,  
37 chlorophyll *a*, temperature, and water mass movements. *Actinobacteria* OTUs showed  
38 particularly strong correlations to bloom dynamics. AcI-C OTUs became more abundant,  
39 while acI-A and acI-B OTUs declined during the bloom, providing evidence of niche  
40 partitioning at the sub-clade level. Thus, our observations in western Lake Erie support a  
41 link between CHABs and disturbances to bacterial community diversity and composition.  
42 Additionally, the short recovery of many taxa after the bloom indicates that bacterial  
43 communities may exhibit resilience to CHABs.

44

45

46

47

48 **Originality-Significance Statement (not to appear in published manuscript).**

49 CHABs are a global threat to freshwater resources. Case in point was western  
50 Lake Erie's 2014 CHAB that resulted in a drinking water shutdown in Toledo, Ohio,  
51 impacting 500,000 residents. Using weekly time-resolved molecular data, we describe the  
52 community ecology of *Cyanobacterial* taxa during this bloom, and we demonstrate how  
53 the bloom corresponded to shifts in bacterial diversity and composition. This work  
54 contributes to our understanding of how CHABs affect microbial communities, and it  
55 also contributes to a broader literature on disturbance and resilience of microbial  
56 communities.

57  
58 **Introduction.**

59 Cyanobacterial harmful algal blooms (CHABs) are a major threat to freshwater  
60 ecosystems globally and are primarily driven by human activities (Paerl and Huisman,  
61 2009; O'Neil *et al.*, 2012; Michalak *et al.*, 2013; Visser *et al.*, 2016). CHABs impact  
62 ecosystems and human health by diminishing habitat for plants and animals, disrupting  
63 food web dynamics, creating hypoxic zones, and producing toxins (Carmichael *et al.*,  
64 2001; Conroy *et al.*, 2005; Hernández *et al.*, 2009; Miller *et al.*, 2010; Backer *et al.*,  
65 2013). Despite a large body of CHAB research (Paerl and Otten, 2013; Steffen *et al.*,  
66 2014; Davis and Gobler, 2016), relatively few studies have examined this phenomenon  
67 from a microbial ecology perspective that includes the community ecology of dominant  
68 cyanobacterial species as well as associations between cyanobacterial populations and  
69 other bacterial populations, which we will refer to as "nc-bacterial".

70 CHAB cyanobacterial diversity can vary both spatially and temporally within a  
71 lake. For example, a year-long study from Yanga Lake (Australia) found a succession of  
72 cyanobacterial consortia through time, which was determined by seasonal biotic and  
73 abiotic fluxes (Woodhouse *et al.*, 2015). In another example, a study from western Lake  
74 Erie (USA) found that *Microcystis* dominated in low P:N locations, while *Anabaena* and  
75 *Planktothrix* dominated in high P:N locations, because *Microcystis* was better able to  
76 scavenge phosphorus (Harke, Davis, *et al.*, 2016). While prior studies have investigated  
77 some of the spatiotemporal trends of CHAB communities, we lack insight into how these  
78 communities vary on highly resolved time scales. Increased temporal resolution of  
79 CHAB community datasets may elucidate additional ecological associations between  
80 CHAB species that are key to understanding bloom ecology.

81 Another important aspect of CHAB ecology is the extent to which these events  
82 impact nc-bacterial communities. We currently have poor understanding of if and how  
83 CHABs influence nc-bacterial richness and evenness (alpha diversity). Field studies from  
84 Lake Taihu (China) found no effect on bacterial alpha diversity (Tang *et al.*, 2010;  
85 Wilhelm *et al.*, 2011), while a study from Yanga Lake found that diversity increased with  
86 cyanobacterial biovolume (Woodhouse *et al.*, 2015). These conflicting results could  
87 possibly be explained by differential responses between bacterial groups. In a study using  
88 pond mesocosms, the richness of bacterial groups were shown to have strikingly different  
89 responses to experimentally manipulated primary productivity measured by chl *a*  
90 (Horner-Devine *et al.*, 2003). Specifically, *Alphaproteobacteria* exhibited a negative  
91 unimodal relationship, *Bacteroidetes* exhibited a positive unimodal relationship, and  
92 *Betaproteobacteria* exhibited no relationship to chl *a* concentrations. Therefore, analysis

93 within taxonomic groups may help clarify the influence of CHABs on nc-bacterial alpha  
94 diversity.

95 Similarly, CHABs are known to influence the composition of bacterial  
96 communities, but again, prior studies have reported conflicting results. A study from  
97 Lake Taihu found that bacteria attached to organic aggregates were different between two  
98 sites with differing chl *a* concentrations (Tang *et al.*, 2010), but they also reported strong  
99 influences of co-varying factors such as temperature, oxygen, turbidity, and inorganic  
100 nutrients. Meanwhile, a study from Yanga Lake reported that bacterial community  
101 composition was influenced by pH, temperature, oxygen, and conductivity during a  
102 CHAB (Woodhouse *et al.*, 2015). Therefore, the relative impacts of CHABs versus  
103 abiotic factors on nc-bacterial community composition are still unclear.

104 To address these outstanding questions in CHAB microbial ecology, we  
105 investigated spatiotemporal dynamics of cyanobacterial populations, as well as changes  
106 to nc-bacterial alpha diversity and composition during the 2014 western Lake Erie  
107 CHAB. Lake Erie is the twelfth largest freshwater lake on Earth by surface area (Ohio  
108 Department of Natural Resources). It also provides essential ecosystem services by  
109 supporting a \$1 billion USD fishing economy and supplying drinking water to over 11  
110 million people (Ohio Department of Natural Resources; Bingham *et al.*, 2015). The  
111 CHAB in 2014 is of particular relevance, because it led to the drinking water crisis in  
112 Toledo, Ohio (Tanber, 2014). Insights into freshwater bacterial community ecology  
113 during CHAB events can point us towards possible interactions between cyanobacterial  
114 species that govern CHAB development and termination, and it can also inform

115 predictions of nc-bacterially-mediated ecosystem processes during these high impact  
116 disturbances.

117

## 118 **Results and Discussion.**

### 119 *Bloom diversity, toxicity, and ecology*

120 A CHAB occurred in western Lake Erie between late July and late October of  
121 2014, characterized by elevated algal pigments (chl *a* and phycocyanin) and elevated  
122 particulate microcystin cyanotoxins (Figure 1b). We observed the bloom at three sites:  
123 the two nearshore sites, situated near the Maumee River, had higher median chl *a*  
124 concentrations than the offshore site (Figure 1a; Nearshore1 median: 18.5, Nearshore 2:  
125 13.72, Offshore median: 5.86). However, the range of pigment values at each site was  
126 large, so on certain dates e.g., first August time point (Aug. 4) and first and second  
127 September time points (Sept. 2, Sept. 8), the offshore site had similarly high levels as  
128 nearshore sites. In later analyses, we leverage these temporal differences in bloom  
129 intensity between nearshore and offshore sites to model variation in nc-bacterial  
130 composition associated with the bloom.

131 Chl *a* and phycocyanin concentrations measured at the same site and date were  
132 highly correlated ( $p < 0.001$ , Spearman's  $\rho = 0.793$ ). Correlations between time-series  
133 can result in spurious results (Johansen, 2007), but visual inspection indicated that the  
134 two variables were qualitatively correlated (Figure 1b). Since chl *a* is produced by most  
135 phytoplankton, but phycocyanin is only produced by *Cyanobacteria*, this analysis  
136 suggests that *Cyanobacteria* dominated the bloom dynamics. However, these data do not  
137 preclude the presence of eukaryotic phytoplankton species. In fact, our universal 16S

138 primers picked up numerous chloroplast reads, suggesting that eukaryotic species were  
139 present. Eukaryotic algae were not the focus of this study, so they were removed from the  
140 dataset.

141 Particulate microcystin toxin was correlated with phycocyanin concentrations ( $p <$   
142  $0.001$ , Spearman's  $\rho = 0.836$ ), but this relationship differed qualitatively between early  
143 and late bloom periods (Figure 1b). From mid-July to late August, elevated phycocyanin  
144 corresponded to high levels of particulate microcystin. Then from early September to  
145 October, elevated phycocyanin corresponded to lower toxin concentrations. Despite this  
146 shift in toxicity, there was a single dominant *Microcystis* OTU present in the community  
147 (Figure 2b). These data can be explained by the fact that there are numerous *Microcystis*  
148 strains that have more than 97% similarity in their full-length 16S rRNA gene, yet differ  
149 with respect to toxigenic potential and other ecological traits (Harke, Steffen, *et al.*,  
150 2016).

151 The cyanobacterial community was a diverse community of 11 non-rare OTUs  
152 (mean relative abundance  $> 0.05$  %) assigned to *Synechococcus*, *Microcystis*, unclassified  
153 genera, *Pseudanabaena*, and *Anabaena* (in order of mean relative abundance) (Figure 2a,  
154 2b). Prior studies of CHABs on Lake Erie have primarily used microscopy to identify  
155 cyanobacterial species, and have reported that *Microcystis* was the heavily dominant  
156 cyanobacterium by biomass (Bridgeman *et al.*, 2013; Michalak *et al.*, 2013; Steffen *et al.*,  
157 2014; Harke, Davis, *et al.*, 2016). In contrast, our molecular data indicates that the 2014  
158 CHAB consisted of a more diverse cyanobacterial community that varied highly in  
159 composition over space and time. *Synechococcus* initiated the bloom at all three sites, and  
160 remained an abundant genus (by gene copy abundance) throughout the entirety of the

161 bloom. However, once *Microcystis* rose to abundance (3-4 weeks after *Synechococcus*), it  
162 dominated at the nearshore stations, while *Synechococcus* continued to dominate at the  
163 offshore station (Figure 2a).

164 Only a few studies have discussed the abundance and importance of  
165 *Synechococcus* in Lake Erie's CHABs (Ouellette *et al.*, 2006; Gobler *et al.*, 2008; Davis  
166 *et al.*, 2012). This discrepancy could be related to either a predefined focus on  
167 *Microcystis* (e.g., using *Microcystis* specific primers), or a bias against picobacteria  
168 during sampling and morphological identification (e.g., colony-only sampling or a focus  
169 on the higher biomass per cell of colonial and filamentous *Cyanobacteria*). However,  
170 *Synechococcus* species likely co-occur with *Microcystis* in several systems, because a  
171 molecular-based study on Lake Taihu found that *Synechococcus* was abundant during  
172 *Microcystis* blooms (Ye *et al.*, 2011). We observed both positive and negative  
173 correlations between *Microcystis* and *Synechococcus* OTUs in our study, though only one  
174 correlation between *Microcystis* and *Synechococcus* OTU 177 was significant (Table S1).  
175 Still, the persistent dominance of *Synechococcus* at the offshore station, where  
176 *Microcystis* abundance was generally lower, suggests that there may be a competitive or  
177 antagonistic interaction between these taxa. In fact, microcystin has been shown to inhibit  
178 the growth of some *Synechococcus* species (Hu *et al.*, 2004). Future experimental studies  
179 might address how ecological interactions with *Microcystis* vary among different  
180 *Synechococcus* taxa.

181 *Pseudanabaena* was the third most abundant genus, and like *Microcystis*, we only  
182 detected one abundant OTU (Figure 2b). *Pseudanabaena* co-occurred with *Microcystis*  
183 throughout much of the bloom, and the relative abundances of the two were highly

184 correlated (Table S1). Previous studies have shown that *Pseudanabaena* can be epiphytic  
185 on *Microcystis* colonies (Agha *et al.*, 2016), therefore it is not surprising that these two  
186 genera would be correlated. Furthermore, some *Pseudanabaena* strains have the genetic  
187 potential to produce cyanotoxins (Rangel *et al.*, 2014), thus co-occurrence of  
188 *Pseudanabaena* and *Microcystis* may have repercussions for CHAB toxicity.

189 Finally, observed dynamics of *Anabaena* and *Microcystis* support prior  
190 hypotheses addressing the competitive advantages of either genus under different nutrient  
191 regimes. *Anabaena* and *Microcystis* were not significantly anti-correlated (Table S1), but  
192 their opposing relationship was qualitatively apparent. For example, *Anabaena* was  
193 mostly absent from the Erie basin in the first stage of the bloom when phosphorus  
194 concentrations were low (Figure 2a, Figure S1). However, in late summer, when  
195 phosphorus levels increased and dissolved inorganic nitrogen concentrations decreased,  
196 *Anabaena* reached its peak level relative to *Microcystis*, particularly at the offshore site.  
197 These patterns are consistent with previous findings that *Microcystis* upregulates P-  
198 scavenging genes and outcompetes *Anabaena* in P-limited environments (Gobler *et al.*,  
199 2016; Harke, Davis, *et al.*, 2016).

200 One major caveat to the observations described above, as well as correlations  
201 made between taxa in the rest of this paper, is that these associations are biased in several  
202 ways by extraction protocol, primers, and the compositional nature of sequence data  
203 (Aitchison, 1982; Brooks *et al.*, 2015). The universal primer set we used is known to be  
204 biased against SAR11, an *Alphaproteobacteria* common in marine environments, which  
205 has a sister lineage (LD12) that is ubiquitous in freshwater systems (Apprill *et al.*, 2015).  
206 Furthermore, a correlation does not imply causality or even interaction. Still, these

207 observations can be quite informative when considered in the context of other  
208 observational and laboratory data.

209 In summary, the cyanobacterial community in western Lake Erie's 2014 CHAB  
210 was diverse and highly dynamic at the OTU level. The community was spatially  
211 heterogeneous, such that *Synechococcus* and *Anabaena* were more abundant offshore and  
212 *Microcystis* dominated near to shore. In addition, weekly temporal sampling revealed  
213 putative associations between cyanobacterial taxa, which could form the basis for more  
214 specific experimental studies examining pairwise ecological interactions.

215

#### 216 *Seasonal and bloom-associated patterns in nc-bacterial alpha diversity*

217 Nc-bacterial richness and evenness exhibited differing temporal dynamics during  
218 the bloom cycle. With the exception of a few highly variable samples in October,  
219 observed nc-bacterial richness increased throughout the season (Figure 3A). In contrast,  
220 nc-bacterial evenness, measured by Simpson's E, decreased until October (Figure 3E). It  
221 should be noted that rarefaction curves of OTU richness rarely reach saturation in diverse  
222 microbial environments, so richness estimates are highly dependent on sequencing depth.  
223 Therefore, we reported our estimates as observed richness (out of 15,631 sequences)  
224 rather than true richness. Still, our richness estimates show consistent trends with other  
225 studies that have observed increasing bacterial diversity from the spring to early fall in  
226 freshwater systems (Shade *et al.*, 2007; Kara *et al.*, 2012) and in the surface waters of  
227 marine systems (Cram *et al.*, 2015).

228 We did not observe a relationship between algal pigments and nc-bacterial  
229 richness (Figure 3B-D, Figure S2); however, we did find relationships between algal

230 pigments and the evenness of certain taxonomic groups (Figure 3F-H, Figure S2).  
231 *Alphaproteobacteria* evenness exhibited a unimodal response to log chl *a*, while  
232 *Bacteroidetes* evenness exhibited a linear response. The evenness of *Betaproteobacteria*  
233 was also slightly positively correlated with log chl *a*, though the association was not  
234 strong enough to be certain. However, the Inverse Simpson Index, which combines both  
235 richness and evenness, showed a much stronger response for linking log chl *a* to  
236 *Betaproteobacteria* ( $p < 0.001$ ,  $R^2 = 0.328$ ). Therefore, this analysis is quite sensitive to  
237 the measure of alpha diversity used.

238         In general, our data suggest that the bloom influences bacterial evenness more  
239 than bacterial richness. We hypothesize that increases in the evenness of dominant  
240 bacterial groups during the CHAB could be related to an increase in habitat complexity  
241 (colony-attached communities) or substrate complexity (carbon compounds from a  
242 diverse algal community), which would allow rare or dormant taxa to become relatively  
243 more abundant. While bloom specialists might be expected to dominate during this  
244 period, rapid weekly shifts in algal abundance (assumed from changes in pigments) and  
245 cyanobacterial composition could inhibit this, thereby promoting a more even  
246 community.

247         In addition to chl *a*, we investigated the relationship of nc-bacterial richness and  
248 evenness with other measurements of the bloom. Lake pH can increase to very high  
249 levels during cyanobacterial blooms due to heightened primary productivity (López-  
250 Archilla *et al.*, 2004), because photosynthesis fixes carbon and displaces the equilibrium  
251 of carbon dioxide/bicarbonate/carbonate that would otherwise buffer a freshwater system.  
252 Compared to chl *a*, pH showed very similar and slightly stronger trends with respect to

253 evenness of *Alphaproteobacteria* and *Betaproteobacteria* (Figure S3). Chl *a* is often used  
254 as a proxy for primary productivity (Downing and Leibold, 2002; Horner-Devine *et al.*,  
255 2003; Smith, 2007), but light, nutrients, and grazing rates can decouple the two by  
256 affecting per cell concentrations of chlorophyll or by reducing the standing stock of  
257 phytoplankton (Behrenfeld *et al.*, 2005). Lake pH can be affected by geochemical  
258 conditions e.g., salt concentrations and presence of mineral carbonates, but there is no  
259 evidence for these conditions changing rapidly in western Lake Erie during the summer  
260 season. Therefore, pH might be a better proxy for primary productivity than chl *a* in this  
261 system, and would consequently correspond more strongly to bacterial diversity if such a  
262 relationship exists. Phycocyanin showed similar trends to nc-bacterial evenness (Figure  
263 S3), but the relationships were weaker, which suggests that nc-bacterial evenness is more  
264 affected by the total algal community than solely *Cyanobacteria*.

265 Our data, supporting a link between the bloom and evenness of certain bacterial  
266 taxa, are consistent with experimental evidence that primary productivity affects alpha  
267 diversity of bacterial groups in different ways (Horner-Devine *et al.*, 2003). However, the  
268 actual relationships we observed were quite distinct for each taxonomic group.  
269 Specifically, *Alphaproteobacteria* exhibited a U-shaped response to chl *a* in a pond  
270 mesocosm study (Horner-Devine *et al.*, 2003), but our study shows the inverse hump-  
271 shape. The mesocosm study found a hump-shaped response for *Betaproteobacteria*, but  
272 we found a positive linear trend. Discrepancies between these studies could be due to  
273 differences in community composition, differences in the range of chl *a* levels over which  
274 the communities were sampled, or other environmental factors that differ between a field  
275 and lab environment. Our results also differ from other CHABs field studies that have

276 found no effect of the bloom on bacterial alpha diversity (Eiler and Bertilsson, 2004;  
277 Woodhouse *et al.*, 2015), though these studies only examined total bacterial richness. In  
278 lieu of our findings, future studies should examine both bacterial richness and evenness,  
279 and should explore diversity patterns within major taxonomic groups.

280 This study provides some initial data differentiating between how annual cycles  
281 and bloom-associated trends affect the richness and evenness of freshwater nc-bacterial  
282 groups. Future studies that expand our observations across multiple years and cover the  
283 full annual range of seasonal variation will further resolve the intertwined effects of  
284 seasonality and CHABs growth dynamics on bacterial alpha diversity.

285

#### 286 *Influence of CHABs and abiotic seasonal factors on nc-bacterial community composition*

287 The nc-bacterial community exhibited large shifts in composition during the 2014  
288 bloom cycle. The Bray-Curtis dissimilarities between the first June samples and peak  
289 bloom dates in August or September were 0.784, 0.812, and 0.642 for nearshore1,  
290 nearshore2, and offshore respectively. We expected that several biotic and abiotic factors  
291 contributed to these fluctuations, so rather than examining several factors independently,  
292 we used principal coordinates to identify the major axes of variation within the  
293 community. We then determined which variables corresponded to change across each  
294 axis over time with linear time-series models. In considering each principal coordinate,  
295 we examined whether sample scores were similar between nearshore and offshore sites.  
296 Abiotic seasonal dynamics should influence all three stations similarly, while the CHAB,  
297 if it has an effect, should influence the offshore site differentially than the nearshore sites  
298 on dates with large discrepancies in bloom intensity. We considered three principal

299 coordinates, because the third coordinate was situated at an obvious inflection point of  
300 the scree plot for relative variance explained by each axis (Figure S4).

301 The first principal coordinate (PC1) of Bray-Curtis sample dissimilarities  
302 explained 34.8% of variation in nc-bacterial community composition across all samples.  
303 PC1 scores exhibited a hump-shaped response over time, which was highly consistent for  
304 the two nearshore sites, but showed differences between nearshore and offshore sites in  
305 mid August and mid to late September (Figure 4A). These differences corresponded to  
306 dates when algal pigments were considerably lower at the offshore station than nearshore  
307 stations (Figure 1B), suggesting that the bloom could be an influencing factor. We  
308 attempted to model PC1 scores solely with environmental data, but we achieved much  
309 better results when time was included as an additional covariate. The best model included  
310 time and pH, though the model with time and chl *a* had a similar  $R^2$  value (Table 1). For  
311 the model including pH, residuals were normal and did not exhibit autocorrelation  
312 (Figure S5), indicating that model assumptions were met. Model cross-validation  
313 returned a low mean squared error, indicating that the model was highly predictive.

314 We posit that PC1 reflects changes in composition associated with the bloom and  
315 other seasonal factors. pH and chl *a* were the two strongest environmental predictors of  
316 PC1, and they can both serve as measures of bloom intensity. pH increases during blooms  
317 because algal photosynthesis removes carbon dioxide from the water and increases  
318 hydroxide ion concentration. In our sampling season, pH reached exceedingly high levels  
319 for a lake (>9, Figure S2), which is indicative of very high primary productivity in an  
320 otherwise well-buffered system (López-Archilla *et al.*, 2004). Our model also suggests  
321 that seasonal variation is important, because the model fit improved considerably when

322 time was added as a covariate. Due to the limited interval of our study, it is difficult to  
323 interpret the meaning of the time variable. We think it's likely that there is a sinusoidal  
324 seasonal trend, but it appears as a linear trend during this four-month period.

325         There are multiple mechanisms by which an algal bloom can affect bacterial  
326 community composition. A shift from allochthonous to autochthonous dissolved organic  
327 carbon was observed during this CHAB (Cory *et al.*, 2016), which may have influenced  
328 the relative abundance of different taxa. Several other studies have documented that  
329 bacterial communities respond to shifts in substrates available within the dissolved  
330 organic carbon pool during both freshwater and marine blooms (Lau *et al.*, 2007; Teeling  
331 *et al.*, 2012; Yang *et al.*, 2015). Alternatively, pH is known to be a major influence on  
332 bacterial community composition in soil (Lauber *et al.*, 2009) and freshwater systems  
333 (Lindstrom *et al.*, 2005; Llíros *et al.*, 2014). Therefore, the bloom may have actually  
334 influenced the composition of nc-bacterial communities by changing the lake's pH. pH  
335 was found to be the most important factor structuring bacterial communities across 15  
336 North European lakes spanning the range of 5.5 to 8.7 (Lindstrom *et al.*, 2005), and in  
337 Tibetan lake sediments spanning the range of 6.88 to 10.37 (Xiong *et al.*, 2012). The pH  
338 range in our study spanned from 7.9 to 9.3, which is smaller than other studies, but may  
339 have covered critical thresholds. Importantly, the correlation of pH with PC1 suggests  
340 that changes to community composition were not driven solely by the presence of  
341 *Cyanobacteria* or harmful cyanobacterial species, but rather by the cumulative properties  
342 of the bloom, which would include eukaryotic or non-harmful species. If this is true,  
343 CHABs may not be particularly distinct disturbances to bacterial communities from other  
344 phytoplankton blooms that reach the same magnitude of primary productivity.

345           The second principal coordinate represented 11.0 % of the variation in nc-  
346 bacterial community composition, which was less than one-third of the variation  
347 explained by PC1. Unlike PC1, sample scores on PC2 were highly similar between  
348 nearshore and offshore sites on all dates (Figure 4C). Therefore, it is unlikely that bloom-  
349 related factors were strongly correlated to this axis of variation. Temperature was the best  
350 predictor of PC2 scores (Table 1). We did not include time as a covariate, because time  
351 was highly correlated with temperature, and it created multicollinearity issues in our  
352 model. The temperature model residuals were normal, and did not exhibit significant  
353 autocorrelation (Figure S5). However, cross-validation returned a somewhat high mean  
354 squared error, indicating that model estimates could still be biased by temporal trends for  
355 which we didn't account. Nevertheless, our model supports that temperature was an  
356 important factor in the structuring of nc-bacterial community composition. Congruently,  
357 freshwater bacterial communities are known to undergo seasonal shifts, and temperature  
358 has been found to be the single largest determinant of these patterns (Kent *et al.*, 2004;  
359 Crump and Hobbie, 2005; Shade *et al.*, 2007).

360           Finally, PC3 explained only 6.72% of variation in nc-bacterial community  
361 composition. PC3 scores differed strongly between nearshore and offshore sites, but  
362 unlike PC1, these differences did not correspond to dates with large discrepancies in  
363 bloom intensity (Figure 4E). Conductivity was the best predictor of PC3 scores (Table 1),  
364 and most model assumptions regarding normal independent residuals were met, though  
365 there was some autocorrelation in the residuals from nearshore1 (Figure S5). The Detroit  
366 and Maumee rivers are known to have distinct conductivity signatures (Millie *et al.*).  
367 Therefore, we interpret variation on this third axis as driven primarily by differences in

368 water mass, which result from differential inputs of the Maumee and Detroit rivers to  
369 nearshore and offshore sites.

370 Thus, using three principal coordinates, which together explain more than half of  
371 the variation in nc-bacterial community composition, we identified pH, chl *a*,  
372 temperature, and conductivity as key environmental gradients. PC1, which explained  
373 more than three times the variance of the second and third coordinates, showed evident  
374 differentiation between nearshore and offshore sites on dates with large differences in pH  
375 and chl *a*. Therefore, we argue that the bloom was a considerable disturbance to nc-  
376 bacterial community composition.

377

378 *Bloom effects on abundant nc-bacterial groups and resilience of bacterial communities to*  
379 *CHAB disturbances*

380 Principal coordinates analysis revealed that bloom-associated measures  
381 corresponded to changes in nc-bacterial community composition, but it did not reveal  
382 which taxa were most affected. Therefore, we investigated which nc-bacterial taxa  
383 significantly correlated with shifts in pH and chl *a*. Using Spearman's rank correlation  
384 tests, we found 34 abundant OTUs (mean relative abundance > 0.1%) that were  
385 positively correlated with pH and 27 that were negatively correlated (Table S2). There  
386 was considerable overlap (83%) with the OTUs associated with chl *a*. A majority of the  
387 most significant positive and negative correlated taxa to both bloom measures were  
388 *Actinobacteria* acI OTUs. *Actinobacteria* acI was also the most abundant clade in the nc-  
389 bacterial community by at least three-fold. Interestingly, acI-A and acI-B OTUs  
390 decreased during the CHAB, while acI-C OTUs increased (Figure 5). In addition,

391 changes in the relative abundance of these OTUs differed between nearshore and offshore  
392 stations, particularly on dates in mid August when there was a large discrepancy in algal  
393 pigments and pH. These data suggest there was niche partitioning among acI OTUs in  
394 response to the CHAB, which was conserved at the sub-clade level. Numerous other  
395 studies have documented niche and seasonal partitioning patterns in acI sub-clades  
396 (Allgaier and Grossart, 2006; Newton *et al.*, 2011; Eiler *et al.*, 2012), including  
397 partitioning by the ratio of allochthonous to autochthonous carbon (Jones *et al.*, 2009) as  
398 well as by pH (Newton *et al.*, 2007). However, these prior studies focused on partitioning  
399 between acI-A, acI-B, acII, and acIV. We found no published research on the ecology of  
400 acI-C, so further work will be necessary to determine the mechanism by which this sub-  
401 clade benefits from CHABs, and whether this mechanism is distinct from non-CHAB  
402 algal blooms.

403 Other abundant clades such as bacI, betI, bacV, and betIV did not show the same  
404 conserved niche partitioning to the bloom as acI (Figure S7). Within each clade, there  
405 were individual OTUs that appeared to respond positively or negatively during the  
406 bloom, but there were also abundant OTUs whose relative abundance did not strongly  
407 reflect bloom dynamics.

408 Dynamics at the OTU level, particularly among the acI, demonstrate that nc-  
409 bacterial community composition was highly affected by the western Lake Erie CHAB.  
410 Thus, bacterial communities exhibit a high degree of sensitivity to CHAB disturbances  
411 (Shade *et al.*, 2012). Nevertheless, by the end of October, acI OTUs recovered towards  
412 pre-bloom relative abundance. Similarly, PC1 scores returned nearly to pre-bloom levels  
413 and Bray-Curtis dissimilarities between the first and last time points at each site were

414 substantially smaller than the peak levels observed during the bloom (nearshore1: 0.460,  
415 nearshore2: 0.453, offshore: 0.364). This quick recovery toward baseline levels indicates  
416 community resilience (Shade et al. 2012). Freshwater bacterial communities have  
417 previously been shown to be highly resilient to physical and chemical disturbances  
418 (Shade *et al.*, 2011), and our study indicates that the same may be true for biotic  
419 disturbances.

420

#### 421 **Conclusion.**

422 Western Lake Erie's bacterial community exhibited changes in diversity and  
423 composition during the bloom season of 2014. In particular, the evenness of  
424 *Alphaproteobacteria* and *Betaproteobacteria* showed differential responses to algal  
425 pigment levels, suggesting that the bloom affected niche diversity for these phylogenetic  
426 groups. Changes in community composition could be represented in three coordinates,  
427 with the first coordinate associated most strongly with bloom measures, the second  
428 coordinate associated with temperature, and the third coordinate associated with physical  
429 water mass movements. These results support work by others demonstrating that bacterial  
430 communities are impacted by CHABs, and identifies the acI clade as a particularly  
431 affected group. The time resolution of this study also demonstrates that most taxa  
432 affected by the CHAB exhibit resilience by recovering to pre-bloom levels shortly after  
433 the termination of this biological disturbance. A better understanding of the specific  
434 relationships and processes between bacterial diversity and the occurrence and toxicity of  
435 CHABs will be useful given the projected acceleration of CHABs in future years.

436

437 **Experimental Procedures.**

438 *Sample collection*

439 Samples were collected approximately weekly between mid-June and late  
440 October, 2014 from three stations (nearshore1, nearshore2, offshore) in the western basin  
441 of Lake Erie that correspond to NOAA Great Lakes Environmental Research Laboratory  
442 long-term monitoring sites WE12, WE2, WE4 respectively (NOAA-GLERL).  
443 Nearshore1 is closest to the water intake for the city of Toledo, nearshore2 is close to the  
444 mouth of the Maumee River, and the offshore site is on the northeastern edge of the  
445 bloom perimeter (Figure 1a).

446 Physicochemical measurements and microbial samples were obtained from an  
447 integrated 20 L water sample taken between the surface and 1 m above the bottom. The  
448 sample was homogenized by shaking. All station depths ranged between 4-12 m, and the  
449 shallowness of the western basin prevents vertical stratification. Temperature, pH, and  
450 conductivity were measured on deck, and algal pigment, cyanotoxin, and nutrient  
451 measurements were analyzed at NOAA-GLERL using standard techniques (U.S. EPA,  
452 1979). H<sub>2</sub>O<sub>2</sub> measurements were analyzed according to Cory et al. (2016). For microbial  
453 samples, a 2 L subsample was taken from the 20 L sample and rehomogenized. 150 mL  
454 was syringe filtered onto a 0.22 µm Millipore Express Plus filter (EMD Millipore,  
455 Billerica, MA), though on peak bloom dates the filter clogged before the full volume was  
456 filtered. All filter samples were placed into cryovials with 1 ml of RNeasy lysis buffer (Qiagen,  
457 Foster City, CA) and frozen at -80 °C until extraction.

458

459 *DNA Extraction and Sequencing*

460 Filters were thawed at room temperature and, while folded with biomass facing  
461 inwards, rinsed with sterile PBS to remove RNAlater preservative. Filters were incubated  
462 in 100  $\mu$ L Qiagen ATL tissue lysis buffer, 300  $\mu$ L Qiagen AL lysis buffer, and 30  $\mu$ L  
463 proteinase K for 1 hour at 56 °C on a rotisserie (Qiagen, Hilden, Germany). Cells were  
464 lysed by vortexing for 10 minutes. Lysates were homogenized with the Qiashredder  
465 column, and DNA was purified from the filtrate using the Qiagen DNeasy Blood and  
466 Tissue kit according to standard protocol. Extracted DNA was amplified using primer set  
467 515f/806r, which targets the V4 hypervariable regions of the 16S rRNA gene (Bergmann  
468 *et al.*, 2011). The DNA was then sequenced using Illumina MiSeq v2 chemistry 2x250  
469 (500 cycles) at the University of Michigan Medical School. RTA v1.17.28 and MCS  
470 v2.2.0 software were used to generate data. Fastq files were submitted to the NCBI  
471 sequence read archive under BioProject PRJNA318386, SRA accession number  
472 SRP07334.

473

#### 474 *Sequence Filtering and Pre-processing*

475 Mothur V 1.34.3 was used to perform quality control and cluster sequences into  
476 OTUs (Schloss *et al.*, 2009). Sequence processing was performed according to the  
477 Mothur standard operating procedure ([http://www.mothur.org/wiki/MiSeq\\_SOP](http://www.mothur.org/wiki/MiSeq_SOP) accessed  
478 on March 13, 2015). Taxonomy was assigned to sequences using the Wang method  
479 (Wang *et al.*, 2007) with an 80% bootstrap cutoff using the Freshwater Microbial Field  
480 Guide (FWMFG) (Newton *et al.*, 2011). This database resolves clade and sub-clade level  
481 taxonomy for common freshwater taxa and allows our data to be compared to other  
482 freshwater studies. However, the FWMFG lacks certain taxonomic groups such as

483 *Planctomycetes*, so we used the Silva database V119 (Quast *et al.*, 2013) for the  
484 remaining unassigned reads. OTUs were clustered using the average neighbor algorithm  
485 with a 97% similarity threshold. Mothur output files were imported into R V 3.2.2 (R  
486 Core Team, 2015) using the phyloseq package V 1.10 (McMurdie and Holmes, 2013) for  
487 all downstream analyses of diversity and community composition. All scripts, mother  
488 output files, and sample data are publically available at  
489 <https://github.com/DenefLab/chab-ecology>.

490

#### 491 *Spatial and temporal bloom dynamics*

492 Spearman's correlation tests were used to determine if there were monotonic  
493 relationships between algal pigments, toxin, and pH. To explore positive and negative  
494 associations between Cyanobacteria OTUs, we performed pairwise Spearman's  
495 correlation tests between all OTUs with mean relative abundance > 0.0005 using the  
496 `corr.test` command in the `psych` package with `fdr` correction (Revelle, 2015).

497

#### 498 *Bacterial alpha diversity*

499 Alpha diversity was estimated using observed OTU richness and Simpson's  
500 Evenness (Simpson's E), which is the Inverse Simpson's Index divided by richness.  
501 Alpha diversity estimates were calculated for each sample by sampling sequences with  
502 replacement to 15,631 reads (the smallest library size) and averaging the measures over  
503 100 trials using the `estimate_richness` command in `phyloseq`. Based on scatterplot  
504 visualization, we ran either linear or polynomial models to predict the richness and  
505 evenness of different bacterial groups from log chl *a* concentrations. Chl *a* measurements

22

506 were log scaled in order to meet assumptions of normal residual terms. P-values for each  
507 model were adjusted with a Benjamini-Hochberg false discovery rate (FDR) correction.

508

#### 509 *Bacterial community composition analyses*

510 Differences in nc-bacterial community composition were calculated using the  
511 Bray-Curtis dissimilarity. Before calculating Bray-Curtis, data was transformed by  
512 scaling the raw proportions of OTUs to the read count of the smallest library (15,631  
513 reads in this study), and rounding to the nearest integer count. This method is equivalent  
514 to the estimated value of averaging counts from repeated rarifying trials, but is more  
515 reproducible and does not contribute additional noise to the dataset (McMurdie and  
516 Holmes, 2014). The relative abundance of an nc-bacterial OTU was measured with  
517 respect to the nc-bacteria rather than the total bacterial community to reduce bias from  
518 changes in the cyanobacterial community. However, this method does not completely  
519 eliminate compositional effects (Aitchison, 1982).

520 To investigate differences in nc-bacterial community composition, we  
521 implemented a principal coordinates analysis. The goal of this analysis was to visualize  
522 similarity between samples in reduced dimensions, and to identify the major axes of  
523 variation in community composition through time. These axes are likely, though not  
524 certain, to correspond with environmental gradients. PCoA and related eigen-analyses  
525 have been implemented with time series data (Freeman *et al.*, 2014; Maurice *et al.*,  
526 2015), and the interpretation is similar to other datasets except the sample scores on each  
527 axis are ordered by time. The percentage of variance explained by each axis was  
528 determined from the axis eigenvalue divided by the cumulative sum of all eigenvalues.

529 As the Bray-Curtis dissimilarity is non-euclidean, some principal coordinates (PCs) had  
530 negative eigenvalues, so we applied a Lingoes correction (Lingoes, 1971). To determine  
531 the number of principal coordinates to examine, we looked for the inflection point in the  
532 scree plot, which displays the relative variance in Bray-Curtis dissimilarity explained by  
533 each coordinate.

534 To investigate gradients that could be associated with changes in bacterial  
535 community composition, we constructed linear models using environmental variables  
536 (e.g. nutrients, temperature, pigments) to predict Bray-Curtis principal coordinate scores.  
537 Time series often contain long-term trends in addition to short-term fluctuations.  
538 Therefore, we experimented with including time as an additional covariate in each model.  
539 We assumed that differences between nearshore and offshore sites were due to  
540 environmental conditions, rather than inherent differences between these sites, so our  
541 models only included fixed effects. Model residuals were examined to determine whether  
542 they met assumptions of normality and independence (i.e. no autocorrelation). To assess  
543 model accuracy, we performed “leave-one-timepoint-out” cross validation of the best  
544 models for each axis and reported the mean squared error. This protocol is similar to  
545 LOOCV, except rather than removing one sample at a time during the model training  
546 stage, we removed all three samples from a given time point. This provided a less biased  
547 estimate of model error, because measurements from the same dates were frequently  
548 similar across sites, and would have reduced the error on the test set.

549 In addition to the simple linear models, we attempted to model each set of  
550 principal coordinates scores with multiple linear regression. We included all  
551 environmental variables as potential covariates and used best subset selection to identify

552 the model that minimized the Bayesian Information Criterion. The BIC penalizes more  
553 complex models in order to optimize the total amount of variance explained while  
554 reducing variables that contribute little explanatory power. Because we had relatively few  
555 data points (53) and many potential covariates (13), we also implemented a bootstrap  
556 analysis, in which we sampled with replacement and refit the models 100 times in order  
557 to determine the stability of a particular predictor. However, even with the bootstrapping,  
558 the results of each model varied depending on the seed value. We found that there was  
559 really only one stable predictor (present in >90% of all bootstrapped models), which is  
560 why we proceeded with simple time series models that included a single environmental  
561 covariate.

562         The principal coordinates approach that we took is an example of an indirect  
563 gradient analysis – gradients are unknown a priori and are estimated by linking  
564 environmental variables to the canonical axes of a sample similarity measure. We also  
565 tried an implementation of direct gradient analysis using redundancy analysis (RDA).  
566 RDA is a constrained version of principal components analysis in which the canonical  
567 axes are linear combinations of the response variables and also relate to the response  
568 variable via multiple linear regression. A time series version of RDA can be implemented  
569 using asymmetric eigenvector maps (AEM) (Baho *et al.*, 2015). Our RDA results  
570 identified the same gradients as our PCoA approach among others. Ultimately, we found  
571 the PCoA approach to be more appropriate, because the variance explained by the  
572 constrained axes was not much more than the unconstrained axes, indicating that the  
573 model was missing some important environmental gradients. In particular, we found it

574 more accurate and intuitive to observe the behavior of nearshore vs. offshore sites over  
575 time in unconstrained ordination space than constrained ordination space.

576 Finally, we performed the same principal coordinate analysis and time series  
577 linear model approach for the cyanobacterial community. However, the principal  
578 coordinates exhibited very noisy trends over time and were not strongly correlated to  
579 specific environmental variables. We also had concerns that the compositional nature of  
580 the OTU counts would lead to stronger biases in these analyses, because the  
581 cyanobacterial community constituted a relatively small proportion of all bacterial reads.  
582 Therefore, we report more descriptive statistics of the cyanobacterial community over  
583 time rather than implementing a model-based approach.

584

585 *OTU-level analysis*

586 To find potential positive or negative associations between nc-bacteria and the  
587 bloom, we performed Spearman's rank correlation tests with pH and chl *a*. We examined  
588 all nc-bacteria OTUs with mean relative abundance larger than 0.1% (107 taxa total)  
589 using the corr.test command from the psych package (Revelle, 2015) with an FDR  
590 correction.

591

## 592 **Acknowledgments.**

593 This work was supported by a grant from the Erb Family Foundation made through the  
594 University of Michigan Water Center and by the Great Lakes Restoration Initiative. RMC  
595 was supported by NSF CAREER award 1351745. We are grateful to the crew from  
596 NOAA-GLERL who assisted with fieldwork. We thank current members of the Deneff,

597 Dick, and Duhaime labs for discussion of the manuscript. We also thank Prof. Kerby  
598 Shedden (University of Michigan) for in depth discussion and consultation on statistical  
599 methods. This manuscript is NOAA-GLERL contribution number XXXX.

600

601 **Conflict of interest.**

602 The authors declare they do not have any competing financial interests in relation to this  
603 work.

604 **Figure Legends:**

605 **Figure 1:** A) Map of sampling locations in western Lake Erie. B) Photosynthetic  
606 pigment, toxin, and relative abundance of *Cyanobacteria* reads across sites and sampling  
607 dates. M denotes a missing sample.

608

609 **Figure 2:** Cyanobacterial spatial and temporal dynamics during the western Lake Erie  
610 CHAB. A) Cyanobacterial genus composition across stations and timepoints. Relative  
611 abundance is measured with respect to the total bacterial community. B) Cyanobacterial  
612 OTU temporal dynamics. OTUs with mean relative abundance  $> 0.0001$  are depicted.  
613 Relative abundance is measured with respect to the total bacterial community.

614

615 **Figure 3:** Nc-bacterial alpha diversity trends. A) Nc-bacterial observed richness trends  
616 over time. B-D) Observed richness of *Alphaproteobacteria*, *Bacteroidetes*, and  
617 *Betaproteobacteria* with respect to log chl *a* concentrations. E) Nc-bacterial evenness  
618 measured by Simpson's E over time. F-H) Evenness of *Alphaproteobacteria*,  
619 *Bacteroidetes*, and *Betaproteobacteria* with respect to chl *a* concentrations. Reported p-

27

620 values underwent FDR correction for multiple hypotheses. For plots of other bacterial  
621 groups and correlation to pH and phycocyanin see figures S2-S3.

622

623 **Figure 4:** Principal coordinates analyses of nc-bacterial Bray-Curtis dissimilarity. Three  
624 principal coordinates were selected based on the output of a scree plot.

625 A-B) PC 1 scores with respect to time and pH. C-D) PC 2 scores with respect to time and  
626 temperature. E-F) PC3 scores with respect to time and water specific conductivity.

627 **Figure 5:** Spatial and temporal dynamics of abundant *Actinobacteria* acI OTUs.

628

629 **Table1:** Regression models to predict scores on Bray-Curtis principal coordinates over  
630 time. The top model(s) for each PC are reported. Only one environmental covariate was  
631 considered in each model, and models were compared with and without time as an  
632 additional covariate. P-values underwent FDR correction. Cross validation was  
633 performed by leaving out all samples from the same timepoint as the test set.

634 Supplementary plots showing model residuals are in Figure S5-S6.

635

Variable	PC1	PC1	PC2	PC3
model	~ pH + time	~logChla + time	~ Temperature	~SpCond
p-value	***	***	***	***
R <sup>2</sup>	0.678	0.658	0.822	0.451
Cross-validation MSE	0.01	0.0233	0.0522	0.0494

636

637

638 **Literature.**

639 Agha, R., del Mar Labrador, M., de los Ríos, A., and Quesada, A. (2016) Selectivity and  
640 detrimental effects of epiphytic *Pseudanabaena* on *Microcystis* colonies.

641 *Hydrobiologia* **777**: 139–148.

642 Aitchison, J. (1982) The Statistical Analysis of Compositional Data. *J. R. Stat. Soc. Ser.*

643 *B* **44**: 139–177.

644 Allgaier, M. and Grossart, H.-P. (2006) Diversity and Seasonal Dynamics of

645 Actinobacteria Populations in Four Lakes in Northeastern Germany. *Appl. Environ.*

646 *Microbiol.* **72**: 3489–3497.

647 Apprill, A., McNally, S., Parsons, R., and Weber, L. (2015) Minor revision to V4 region

648 SSU rRNA 806R gene primer greatly increases detection of SAR11

649 bacterioplankton. *Aquat. Microb. Ecol.* **75**: 129–137.

650 Backer, L., Landsberg, J., Miller, M., Keel, K., and Taylor, T. (2013) Canine Cyanotoxin

651 Poisonings in the United States (1920s–2012): Review of Suspected and Confirmed

652 Cases from Three Data Sources. *Toxins (Basel)*. **5**: 1597–1628.

653 Baho, D.L., Futter, M.N., Johnson, R.K., and Angeler, D.G. (2015) Assessing temporal

654 scales and patterns in time series: Comparing methods based on redundancy

655 analysis. *Ecol. Complex.* **22**: 162–168.

656 Behrenfeld, M.J., Boss, E., Siegel, D.A., and Shea, D.M. (2005) Carbon-based ocean

657 productivity and phytoplankton physiology from space. *Global Biogeochem. Cycles*

658 **19**: 1–14.

659 Bergmann, G.T., Bates, S.T., Eilers, K.G., Lauber, C.L., Caporaso, J.G., Walters, W.A.,

660 et al. (2011) The under-recognized dominance of Verrucomicrobia in soil bacterial

- 661 communities. *Soil Biol. Biochem.* **43**: 1450–1455.
- 662 Bingham, M., Sinha, S.K., and Lupi, F. (2015) Economic benefits of reducing harmful  
663 algal blooms in Lake Erie.
- 664 Bridgeman, T.B., Chaffin, J.D., and Filbrun, J.E. (2013) A novel method for tracking  
665 western Lake Erie *Microcystis* blooms, 2002–2011. *J. Great Lakes Res.* **39**: 83–89.
- 666 Brooks, J.P., Edwards, D.J., Harwich, M.D., Rivera, M.C., Fettweis, J.M., Serrano, M.G.,  
667 et al. (2015) The truth about metagenomics: quantifying and counteracting bias in  
668 16S rRNA studies. *BMC Microbiol.* **15**: 66.
- 669 Carmichael, W.W., Azevedo, S.M., An, J.S., Molica, R.J., Jochimsen, E.M., Lau, S., et  
670 al. (2001) Human fatalities from cyanobacteria: chemical and biological evidence  
671 for cyanotoxins. *Environ. Health Perspect.* **109**: 663–8.
- 672 Conroy, J.D., Edwards, W.J., Pontius, R.A., Kane, D.D., Zhang, H., Shea, J.F., et al.  
673 (2005) Soluble nitrogen and phosphorus excretion of exotic freshwater mussels  
674 (*Dreissena* spp.): Potential impacts for nutrient remineralisation in western Lake  
675 Erie. *Freshw. Biol.* **50**: 1146–1162.
- 676 Cory, R.M., Davis, T.W., Dick, G.J., Johengen, T., Denef, V.J., Berry, M., et al. (2016)  
677 Seasonal dynamics in dissolved organic matter, hydrogen peroxide, and  
678 cyanobacterial blooms in Lake Erie. *Front. Mar. Sci.* **3**: 54.
- 679 Cram, J.A., Chow, C.-E.T., Sachdeva, R., Needham, D.M., Parada, A.E., Steele, J.A., and  
680 Fuhrman, J.A. (2015) Seasonal and interannual variability of the marine  
681 bacterioplankton community throughout the water column over ten years. *Isme J* **9**:  
682 563–580.
- 683 Crump, B.C. and Hobbie, J.E. (2005) Synchrony and seasonality in bacterioplankton

- 684 communities of two temperate rivers. *Limnol. Oceanogr.* **50**: 1718–1729.
- 685 Davis, T.W. and Gobler, C.J. (2016) Preface for special issue on global expansion of  
686 harmful cyanobacterial blooms: Diversity, ecology, causes, and controls. *Harmful*  
687 *Algae*.
- 688 Davis, T.W., Koch, F., Marcoval, M.A., Wilhelm, S.W., and Gobler, C.J. (2012)  
689 Mesozooplankton and microzooplankton grazing during cyanobacterial blooms in  
690 the western basin of Lake Erie. *Harmful Algae* **15**: 26–35.
- 691 Downing, A.L. and Leibold, M.A. (2002) Ecosystem consequences of species richness  
692 and composition in pond food webs. *Nature* **416**: 837–841.
- 693 Eiler, A. and Bertilsson, S. (2004) Composition of freshwater bacterial communities  
694 associated with cyanobacterial blooms in four Swedish lakes. *Environ. Microbiol.* **6**:  
695 1228–1243.
- 696 Eiler, A., Heinrich, F., and Bertilsson, S. (2012) Coherent dynamics and association  
697 networks among lake bacterioplankton taxa. *ISME J.* **6**: 330–42.
- 698 Freeman, J., Vladimirov, N., Kawashima, T., Mu, Y., Sofroniew, N.J., Bennett, D. V., et  
699 al. (2014) Mapping brain activity at scale with cluster computing. *Nat. Methods* **11**:  
700 941–950.
- 701 Gobler, C.J., Burkholder, J.M., Davis, T.W., Harke, M.J., Stow, C.A., and Van de Waal,  
702 D.B. (2016) The dual role of nitrogen supply in controlling the growth and toxicity  
703 of cyanobacterial blooms. *Harmful Algae*.
- 704 Gobler, C.J., Davis, T.W., Deonarine, S.N., Saxton, M.A., Lavrentyev, P.J., Jochem, F.J.,  
705 and Wilhelm, S.W. (2008) Grazing and virus-induced mortality of microbial  
706 populations before and during the onset of annual hypoxia in Lake Erie. *Aquat.*

- 707 *Microb. Ecol.* **51**: 117–128.
- 708 Harke, M.J., Davis, T.W., Watson, S.B., and Gobler, C.J. (2016) Nutrient-Controlled  
709 Niche Differentiation of Western Lake Erie Cyanobacterial Populations Revealed  
710 via Metatranscriptomic Surveys. *Environ. Sci. Technol.* **50**: 604–15.
- 711 Harke, M.J., Steffen, M.M., Gobler, C.J., Otten, T.G., Wilhelm, S.W., Wood, S.A., and  
712 Paerl, H.W. (2016) A review of the global ecology, genomics, and biogeography of  
713 the toxic cyanobacterium, *Microcystis* spp. *Harmful Algae* **54**: 4–20.
- 714 Hernández, J.M., López-Rodas, V., and Costas, E. (2009) Microcystins from tap water  
715 could be a risk factor for liver and colorectal cancer: A risk intensified by global  
716 change. *Med. Hypotheses* **72**: 539–540.
- 717 Horner-Devine, M.C., Leibold, M. a, Smith, V.H., and Bohannan, B.J.M. (2003)  
718 Bacterial diversity patterns along a gradient of primary productivity. *Ecol. Lett.* **6**:  
719 613–622.
- 720 Hu, Z., Liu, Y., and Li, D. (2004) Physiological and biochemical analyses of microcystin-  
721 RR toxicity to the cyanobacterium *Synechococcus elongatus*. *Environ. Toxicol.* **19**:  
722 571–7.
- 723 Johansen, S. (2007) Correlation, regression, and cointegration of nonstationary economic  
724 time series. *Creat. Res. Pap.* **2461**: 0–9.
- 725 Jones, S.E., Newton, R.J., and McMahon, K.D. (2009) Evidence for structuring of  
726 bacterial community composition by organic carbon source in temperate lakes.  
727 *Environ. Microbiol.* **11**: 2463–2472.
- 728 Kara, E.L., Hanson, P.C., Hu, Y.H., Winslow, L., and McMahon, K.D. (2012) A decade  
729 of seasonal dynamics and co-occurrences within freshwater bacterioplankton

- 730 communities from eutrophic Lake Mendota, WI, USA. *ISME J.* **7**: 680–684.
- 731 Kent, A.D., Jones, S.E., Yannarell, A.C., Graham, J.M., Lauster, G.H., Kratz, T.K., and  
732 Triplett, E.W. (2004) Annual Patterns in Bacterioplankton Community Variability in  
733 a Humic Lake. *Microb. Ecol.* **48**: 550–560.
- 734 Lau, W.W.Y., Keil, R.G., and Armbrust, E. V. (2007) Succession and Diel  
735 Transcriptional Response of the Glycolate-Utilizing Component of the Bacterial  
736 Community during a Spring Phytoplankton Bloom. *Appl. Environ. Microbiol.* **73**:  
737 2440–2450.
- 738 Lauber, C.L., Hamady, M., Knight, R., and Fierer, N. (2009) Pyrosequencing-Based  
739 Assessment of Soil pH as a Predictor of Soil Bacterial Community Structure at the  
740 Continental Scale. *Appl. Environ. Microbiol.* **75**: 5111–5120.
- 741 Lindstrom, E.S., Kamst-Van Agterveld, M.P., and Zwart, G. (2005) Distribution of  
742 Typical Freshwater Bacterial Groups Is Associated with pH, Temperature, and Lake  
743 Water Retention Time. *Appl. Environ. Microbiol.* **71**: 8201–8206.
- 744 Lingo, J.C. (1971) Some boundary conditions for a monotone analysis of symmetric  
745 matrices. *Psychometrika* **36**: 195–203.
- 746 Llíros, M., Inceoğlu, Ö., García-Armisen, T., Anzil, A., Leporcq, B., Pigneur, L.-M., et  
747 al. (2014) Bacterial Community Composition in Three Freshwater Reservoirs of  
748 Different Alkalinity and Trophic Status. *PLoS One* **9**: e116145.
- 749 López-Archilla, A.I., Moreira, D., López-García, P., and Guerrero, C. (2004)  
750 Phytoplankton diversity and cyanobacterial dominance in a hypereutrophic shallow  
751 lake with biologically produced alkaline pH. *Extremophiles* **8**: 109–115.
- 752 Maurice, C.F., CL Knowles, S., Ladau, J., Pollard, K.S., Fenton, A., Pedersen, A.B., and

- 753 Turnbaugh, P.J. (2015) Marked seasonal variation in the wild mouse gut microbiota.  
754 *ISME J.* **9**: 2423–2434.
- 755 McMurdie, P.J. and Holmes, S. (2013) phyloseq: An R package for reproducible  
756 interactive analysis and graphics of microbiome census data. *PLoS One* **8**: e61217.
- 757 McMurdie, P.J. and Holmes, S. (2014) Waste not, want not: why rarefying microbiome  
758 data is inadmissible. *PLoS Comput. Biol.* **10**: e1003531.
- 759 Michalak, A.M., Anderson, E.J., Beletsky, D., Boland, S., Bosch, N.S., Bridgeman, T.B.,  
760 et al. (2013) Record-setting algal bloom in Lake Erie caused by agricultural and  
761 meteorological trends consistent with expected future conditions. *Proc. Natl. Acad.*  
762 *Sci.* **110**: 6448–6452.
- 763 Miller, M.A., Kudela, R.M., Mekebri, A., Crane, D., Oates, S.C., Tinker, M.T., et al.  
764 (2010) Evidence for a Novel Marine Harmful Algal Bloom: Cyanotoxin  
765 (Microcystin) Transfer from Land to Sea Otters. *PLoS One* **5**: e12576.
- 766 Millie, D.F., Fahnenstiel, G.L., Dyble, J., Ae, B., Pigg, R.J., Rediske, R.R., et al. Late-  
767 summer phytoplankton in western Lake Erie (Laurentian Great Lakes): bloom  
768 distributions, toxicity, and environmental influences.
- 769 Newton, R.J., Jones, S.E., Eiler, A., McMahon, K.D., and Bertilsson, S. (2011) A guide  
770 to the natural history of freshwater lake bacteria.
- 771 Newton, R.J., Jones, S.E., Helmus, M.R., and McMahon, K.D. (2007) Phylogenetic  
772 ecology of the freshwater Actinobacteria acI lineage. *Appl. Environ. Microbiol.* **73**:  
773 7169–7176.
- 774 O’Neil, J.M., Davis, T.W., Burford, M.A., and Gobler, C.J. (2012) The rise of harmful  
775 cyanobacteria blooms: The potential roles of eutrophication and climate change.

- 776 *Harmful Algae* **14**: 313–334.
- 777 Ohio Department of Natural Resources, D. of G.S. Lake Erie Facts.
- 778 Ouellette, A.J.A., Handy, S.M., and Wilhelm, S.W. (2006) Toxic Microcystis is  
779 widespread in Lake Erie: PCR detection of toxin genes and molecular  
780 characterization of associated cyanobacterial communities. *Microb. Ecol.* **51**: 154–  
781 165.
- 782 Paerl, H.W. and Huisman, J. (2009) Climate change: a catalyst for global expansion of  
783 harmful cyanobacterial blooms. *Environ. Microbiol. Rep.* **1**: 27–37.
- 784 Paerl, H.W. and Otten, T.G. (2013) Harmful Cyanobacterial Blooms: Causes,  
785 Consequences, and Controls. *Microb. Ecol.* **65**: 995–1010.
- 786 Quast, C., Pruesse, E., Yilmaz, P., Gerken, J., Schweer, T., Yarza, P., et al. (2013) The  
787 SILVA ribosomal RNA gene database project: Improved data processing and web-  
788 based tools. *Nucleic Acids Res.* **41**:
- 789 R Core Team (2015) R: a language for statistical computing.
- 790 Rangel, M., Martins, J., Garcia, A., Conserva, G., Costa-Neves, A., Sant’Anna, C., and  
791 de Carvalho, L. (2014) Analysis of the Toxicity and Histopathology Induced by the  
792 Oral Administration of *Pseudoanabaena galeata* and *Geitlerinema splendidum*  
793 (Cyanobacteria) Extracts to Mice. *Mar. Drugs* **12**: 508–524.
- 794 Revelle, W. (2015) psych: Procedures for personality and psychological Research.
- 795 Schloss, P.D., Westcott, S.L., Ryabin, T., Hall, J.R., Hartmann, M., Hollister, E.B., et al.  
796 (2009) Introducing mothur: Open-Source, Platform-Independent, Community-  
797 Supported Software for Describing and Comparing Microbial Communities. *Appl.*  
798 *Environ. Microbiol.* **75**: 7537–7541.

- 799 Shade, A., Kent, A.D., Jones, S.E., Newton, R.J., Triplett, E.W., and McMahon, K.D.  
800 (2007) Interannual dynamics and phenology of bacterial communities in a eutrophic  
801 lake. *Limnol. Oceanogr.* **52**: 487–494.
- 802 Shade, A., Peter, H., Allison, S.D., Baho, D.L., Berga, M., B?rgmann, H., et al. (2012)  
803 Fundamentals of microbial community resistance and resilience. *Front. Microbiol.*  
804 **3**: 1–19.
- 805 Shade, A., Read, J.S., Welkie, D.G., Kratz, T.K., Wu, C.H., and McMahon, K.D. (2011)  
806 Resistance, resilience and recovery: Aquatic bacterial dynamics after water column  
807 disturbance. *Environ. Microbiol.* **13**: 2752–2767.
- 808 Smith, V.H. (2007) Microbial diversity-productivity relationships in aquatic ecosystems.  
809 *FEMS Microbiol. Ecol.* **62**: 181–186.
- 810 Steffen, M.M., Belisle, B.S., Watson, S.B., Boyer, G.L., and Wilhelm, S.W. (2014)  
811 Status, causes and controls of cyanobacterial blooms in Lake Erie. *J. Great Lakes*  
812 *Res.* **40**: 215–225.
- 813 Tanber, G. (2014) Toxin leaves 500,000 in northwest Ohio without drinking water.  
814 *Reuters.*
- 815 Tang, X., Gao, G., Chao, J., Wang, X., Zhu, G., and Qin, B. (2010) Dynamics of organic-  
816 aggregate-associated bacterial communities and related environmental factors in  
817 Lake Taihu, a large eutrophic shallow lake in China. *Limnol. Oceanogr.* **55**: 469–  
818 480.
- 819 Teeling, H., Fuchs, B.M., Becher, D., Klockow, C., Gardebrecht, A., Bennke, C.M., et al.  
820 (2012) Substrate-controlled succession of marine bacterioplankton populations  
821 induced by a phytoplankton bloom. *Science* **336**: 608–11.

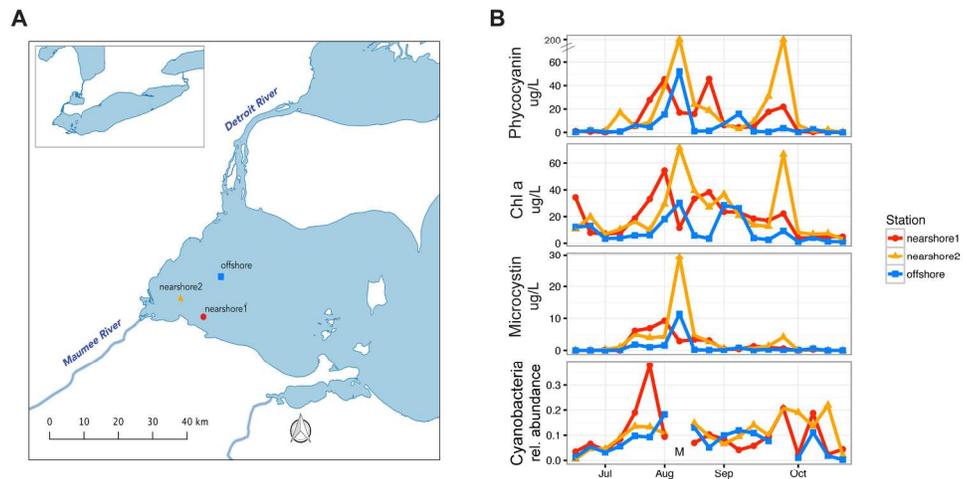
- 822 U.S. EPA (1979) Methods for Chemical Analysis of Water and Wastes Cincinnati, OH.
- 823 Visser, P.M., Verspagen, J.M.H., Sandrini, G., Stal, L.J., Matthijs, H.C.P., Davis, T.W.,  
824 et al. (2016) How rising CO<sub>2</sub> and global warming may stimulate harmful  
825 cyanobacterial blooms. *Harmful Algae* **accepted.**:
- 826 Wang, Q., Garrity, G.M., Tiedje, J.M., and Cole, J.R. (2007) Naive Bayesian Classifier  
827 for Rapid Assignment of rRNA Sequences into the New Bacterial Taxonomy. *Appl.*  
828 *Environ. Microbiol.* **73**: 5261–5267.
- 829 Wilhelm, S.W., Farnsley, S.E., LeCleir, G.R., Layton, A.C., Satchwell, M.F., DeBruyn,  
830 J.M., et al. (2011) The relationships between nutrients, cyanobacterial toxins and the  
831 microbial community in Taihu (Lake Tai), China. *Harmful Algae* **10**: 207–215.
- 832 Woodhouse, J.N., Kinsela, A.S., Collins, R.N., Bowling, L.C., Honeyman, G.L.,  
833 Holliday, J.K., and Neilan, B.A. (2015) Microbial communities reflect temporal  
834 changes in cyanobacterial composition in a shallow ephemeral freshwater lake.  
835 *ISME J.* 1–15.
- 836 Xiong, J., Liu, Y., Lin, X., Zhang, H., Zeng, J., Hou, J., et al. (2012) Geographic distance  
837 and pH drive bacterial distribution in alkaline lake sediments across Tibetan Plateau.  
838 *Environ. Microbiol.* **14**: 2457–2466.
- 839 Yang, C., Li, Y., Zhou, B., Zhou, Y., Zheng, W., Tian, Y., et al. (2015) Illumina  
840 sequencing-based analysis of free-living bacterial community dynamics during an  
841 Akashiwo sanguine bloom in Xiamen sea, China. *Sci. Rep.* **5**: 8476.
- 842 Ye, W., Tan, J., Liu, X., Lin, S., Pan, J., Li, D., and Yang, H. (2011) Temporal variability  
843 of cyanobacterial populations in the water and sediment samples of Lake Taihu as  
844 determined by DGGE and real-time PCR. *Harmful Algae* **10**: 472–479.

845

For Peer Review Only

**Table 1: Regression models to predict scores on Bray-Curtis principal coordinates over time.** The top model(s) for each PC are reported. Only one environmental covariate was considered in each model, and models were compared with and without time as an additional covariate. P-values underwent FDR correction. Cross validation was performed by leaving out all samples from the same timepoint as the test set. Supplementary plots showing model residuals are in Figure S5. MSE = mean squared error.

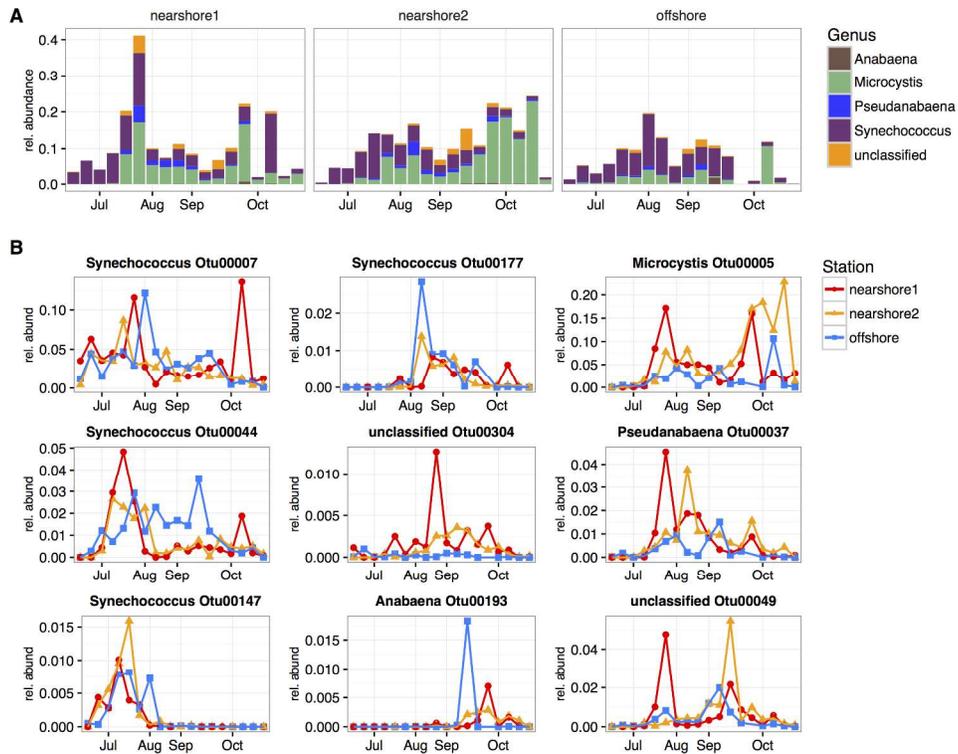
<b>Variable</b>	<b>PC1</b>	<b>PC1</b>	<b>PC2</b>	<b>PC3</b>
model	~ pH + time	~logChla + time	~ Temperature	~SpCond
p-value	<0.001	<0.001	<0.001	<0.001
R <sup>2</sup>	0.678	0.658	0.822	0.451
Cross-validation MSE	0.01	0.0233	0.0522	0.0494



Sample sites and bloom dynamics. (A) Map of sampling locations in western Lake Erie. (B) Photosynthetic pigment, toxin, and relative abundance of Cyanobacteria reads across sites and sampling dates. M denotes a missing sample.

Figure 1  
 216x185mm (300 x 300 DPI)

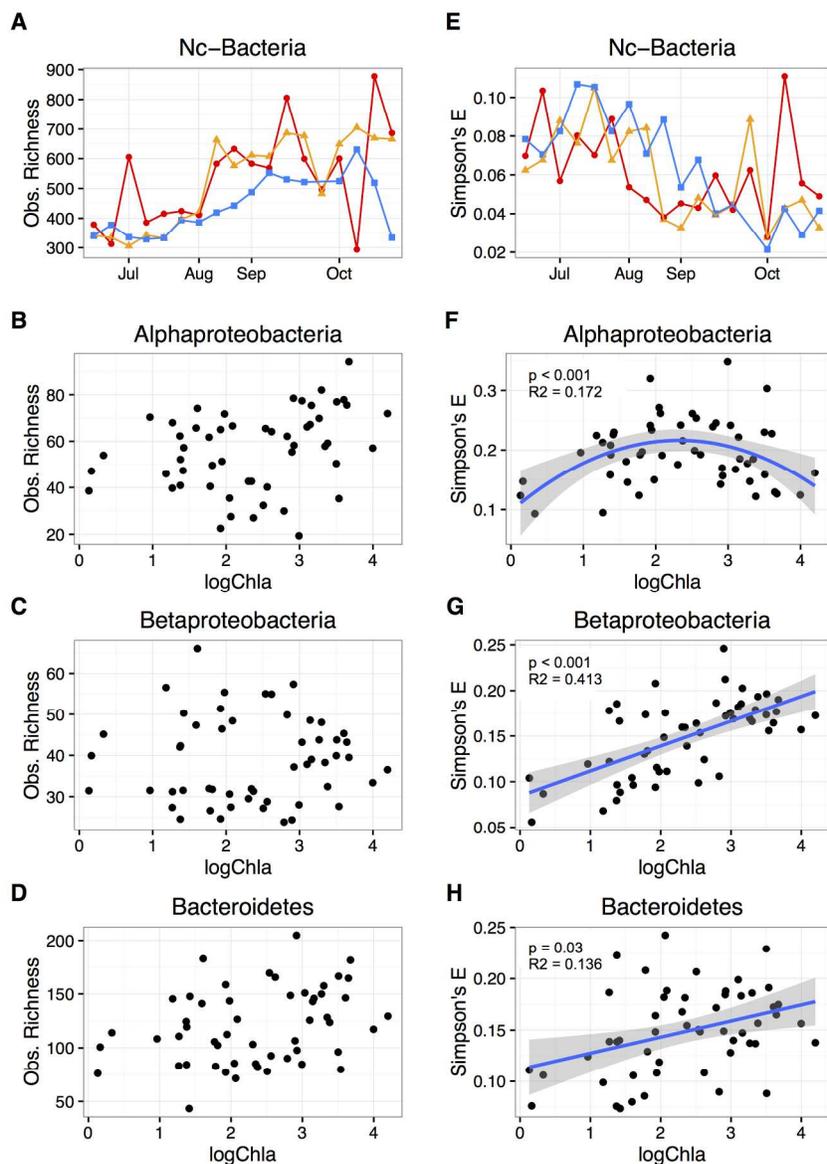
Only



Cyanobacterial spatial and temporal dynamics during the western Lake Erie CHAB. (A) Cyanobacterial genus composition across stations and timepoints. Relative abundance is measured with respect to the total bacterial community. (B) Cyanobacterial OTU temporal dynamics. OTUs with mean relative abundance > 0.0001 are depicted. Relative abundance is measured with respect to the total bacterial community.

Figure 2

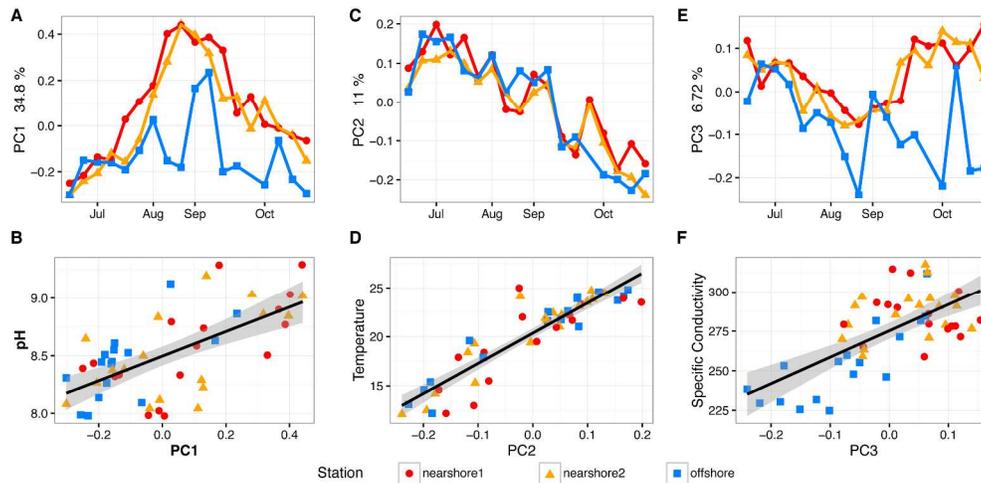
254x203mm (300 x 300 DPI)



Nc-bacterial alpha diversity trends. (A) Nc-bacterial observed richness trends over time. (B-D) Observed richness of Alphaproteobacteria, Bacteroidetes, and Betaproteobacteria with respect to log chl a concentrations. (E) Nc-bacterial evenness measured by Simpson's E over time. (F-H) Evenness of Alphaproteobacteria, Bacteroidetes, and Betaproteobacteria with respect to chl a concentrations. Reported p-values underwent FDR correction for multiple hypotheses. For plots of other bacterial groups and correlation to pH and phycocyanin see figures S2-S3.

Figure 3

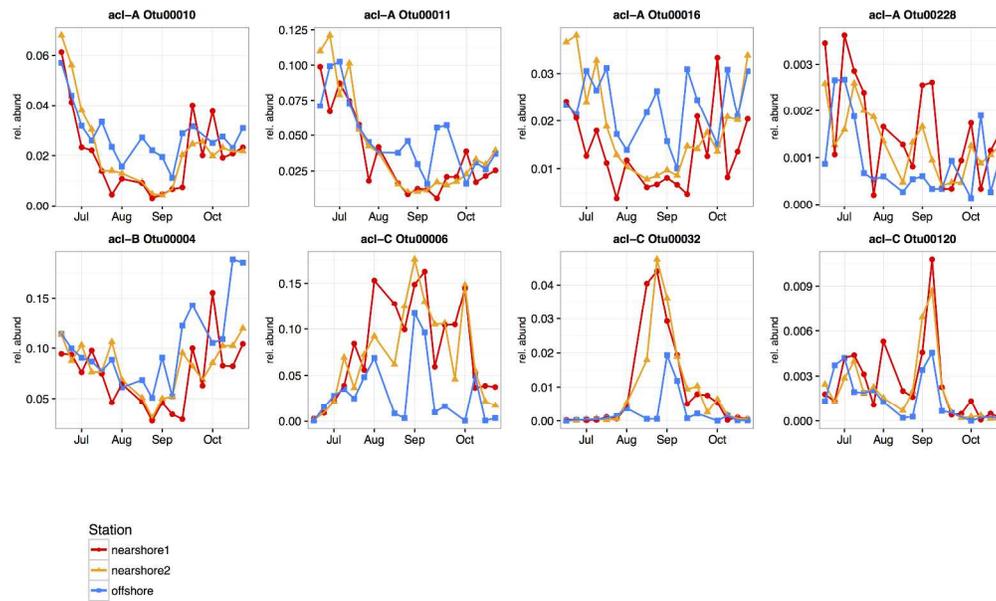
177x254mm (300 x 300 DPI)



Principal coordinates analyses of nc-bacterial Bray-Curtis dissimilarity. Three principal coordinates were selected based on the output of a scree plot (Figure S4).!! † (A-B) PC 1 scores with respect to time and pH. (C-D) PC 2 scores with respect to time and temperature. (E-F) PC3 scores with respect to time and water specific conductivity.!! †

Figure 4

262x126mm (300 x 300 DPI)



Spatial and temporal dynamics of abundant Actinobacteria acI OTUs.

Figure 5

300x179mm (300 x 300 DPI)